Nanotechnology **20** (2009) 255501 (5pp) doi:10.1088/0957-4484/20/25/255501

A gas nanosensor unaffected by humidity

Ting Zhang[1,2], Syed Mubeen[1,2], Bongyoung Yoo[1,2], Nosang V Myung[1,2,4] and Marc A Deshusses[1,2,3,4]

[1] Department of Chemical and Environmental Engineering, University of California-Riverside, Riverside, CA 92521, USA
[2] Center for Nanoscale Science and Engineering, University of California-Riverside, Riverside, CA 92521, USA
[3] Department of Civil and Environmental Engineering, Duke University, Durham, NC 27708, USA

E-mail: myung@engr.ucr.edu and marc.deshusses@duke.edu

Received 12 February 2009, in final form 24 April 2009
Published 2 June 2009
Online at stacks.iop.org/Nano/20/255501

Abstract
The fabrication of a gas nanosensor for detecting ammonia gas in air that is unaffected by humidity is demonstrated. On functionalizing single-walled carbon nanotube (SWNT) networks with a precise amount of camphorsulfonic-acid-doped polyaniline (PANI(CSA)), the opposite electrical resistance responses of the CSA-doped PANI and SWNTs to humid air effectively canceled each other, thereby eliminating any effects of humidity during sensing experiments. The approach should be widely applicable for eliminating undesirable interferences for gas nanosensors.

S Supplementary data are available from stacks.iop.org/Nano/20/255501

(Some figures in this article are in colour only in the electronic version)

1. Introduction

There is increasing demand for low-cost gas sensors that can discriminate between low concentrations of analytes. Nanotechnology offers the promise of improved gas sensors with low-power consumption, fast response time which will enable portability for a wide range of applications. Indeed, nanostructured materials such as nanotubes and nanowires have been shown to be suitable for sensing various gases in a number of recent research reports [1–7]. However, in most cases, these sensors were subject to cross-interferences by other analytes [8–11]. While arraying of nanostructured gas sensing materials combined with advanced numerical methods such as pattern recognition has the potential to filter out interferences [12–15], the development of more analyte specific sensors is desirable.

In the present communication, we demonstrate how the manufacturing of a nanostructured material sensor for ammonia gas can be tuned to eliminate the interference of water vapor. By precisely functionalizing single-walled carbon nanotube (SWNT) networks with camphorsulfonic-acid-doped polyaniline (PANI(CSA)), the opposite electrical responses toward humid air of CSA-doped PANI and SWNTs effectively canceled the humidity interference. The results demonstrate that appropriate selection of nanomaterials and fine tuning of the synthesis conditions can overcome some of the limitations encountered by nanosensors.

2. Experimental methods

Electropolymerization was selected to decorate SWNTs because it is a simple and cost-effective technique which offers spatially-tailored functionalization [7–16]. Electrochemically functionalized PANI(CSA)–SWNT-based sensors were fabricated as follows. First, carboxylated SWNTs (SWNT–COOH 80–90% purity, produced by Carbon Solution, Inc. Riverside) were dispersed (1 μg ml^{-1}) in dimethyl formamide (DMF) with ultrasonication for 1 h. Then, the SWNTs were dispensed across microfabricated gold electrodes (200 μm wide and 3 μm gap) by depositing a 0.1 μl drop of SWNTs solution over the gap using micro-syringe. After evaporation of the DMF solution, a SWNT network was bridging the electrodes to form the sensors. The SWNT–COOH sensors were annealed at 300 °C for 30 min in 99.999% argon to improve the contact between the SWNTs and the gold electrodes. Finally,

[4] Authors to whom any correspondence should be addressed.

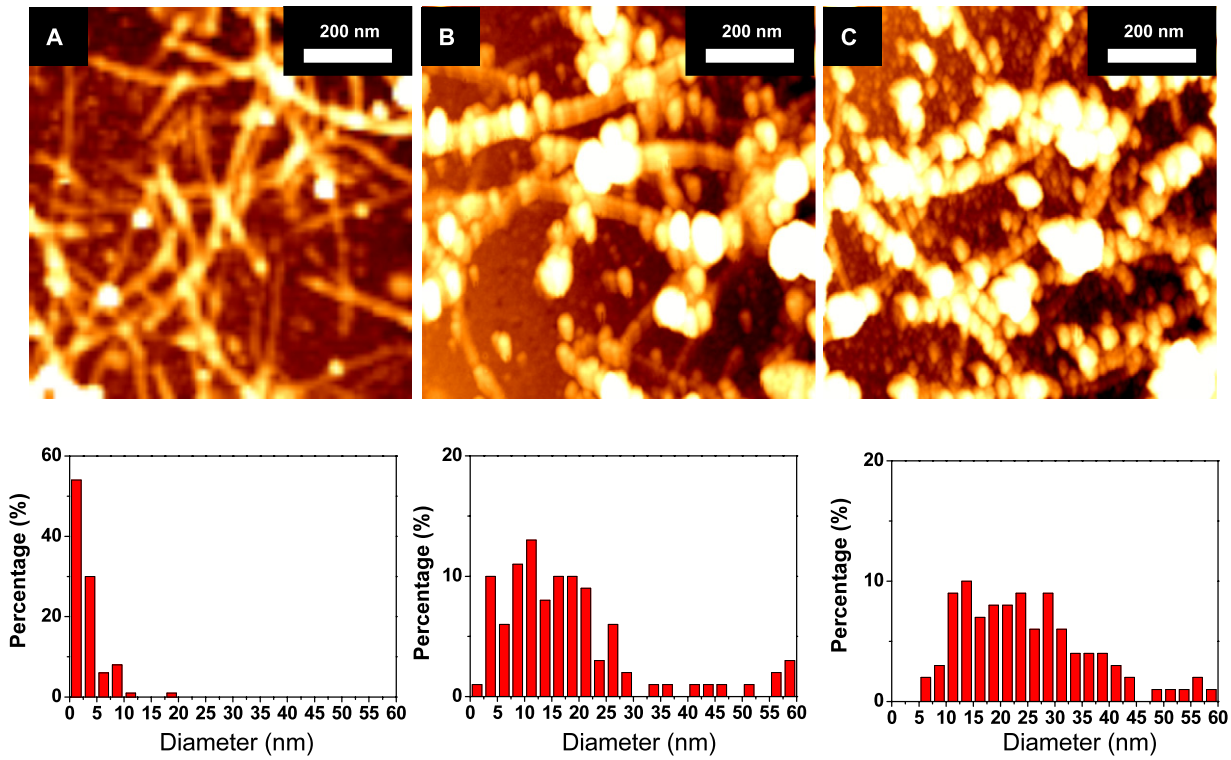

Figure 1. AFM images and diameter histograms of CSA-doped PANI coated SWNT networks as a function of deposition time: (A) bare carboxylated SWNT network, (B) after 2 min PANI deposition, and (C) after 5 min deposition. Each histogram was built from 100 individual SWNTs transects.

electrochemical functionalization was performed with a three-electrode configuration: the SWNT network along with the gold electrodes, a stainless steel tip, and a chlorinated Ag wire were used as the working, counter, and reference electrodes, respectively. 3 μl of a deoxygenated 0.1 M aniline and 0.1 M CSA aqueous solution served as electrolyte and was placed on top of the SWNT network followed by insertion of the counter and reference electrodes. PANI(CSA) was deposited on the SWNTs at a constant potential of 0.8 V versus chlorinated Ag wire. It is hypothesized that COOH moieties on the SWNT act as defect sites where PANI preferentially deposits forming non-covalent bonds with the SWNTs. The PANI(CSA) coating thickness was controlled by adjusting the deposition time.

For electronic characterization of PANI(CSA)–SWNT sensors, I–V characteristics were determined using a semiconducting parameter analyzer (HP 4155A) with potential sweeping from -1 to 1 V. The temperature-dependent electrical properties were characterized using a Physical Property Measurement System (PPMS).

For gas detection studies, the sensors were wired bonded and each sensor was connected in series with a load resistor. The value of the load resistance was chosen to be as close as possible to the resistance of the sensor to optimize the resolution obtained from measurements. 1 VDC potential was applied to the circuit and the electrical resistance of the sensor was determined from continuously monitoring the voltage over the load resistor using Ohm's law. A sealed glass chamber with gas inlet and outlet ports for gas flow-through was positioned over the sensor chip. All experiments were conducted at 24 °C with known concentrations of ammonia diluted in air at a total gas flow of 200 std. cm^3 min^{-1}. Dry and 100% relative humidity air were mixed to achieve the desired relative humidity which was verified using a thermo-hygrometer. The analytes, dry and humid air flow rates were regulated by mass flow controllers (Alicat Scientific Incorporated, Tucson, AZ). A custom Labview computer program served to control and monitor the system (National Instruments, Austin, TX).

3. Results and discussion

The morphology of the PANI(CSA) coated SWNT networks was characterized using an atomic force microscope (PSIA, Inc.). AFM images and diameter histograms of PANI(CSA) coated SWNTs revealed nodular polymer deposits on the SWNTs (figure 1). The average diameter of the PANI(CSA)–SWNT composite increased from 3.3 nm before PANI deposition indicating that the network was mostly made of monodispersed SWNTs, to 17 and 23 nm with increasing the PANI deposition time to 2 and 5 min, respectively. At intermediate electropolymerization time (figure 1(B)), about 10% of the SWNT surface remained unfunctionalized by PANI. Cyclic voltammetry in 1 M NaCl confirmed the deposition of PANI (data not shown).

Temperature-dependent I–V curves showed a nonlinear 'S' shape, with nonlinearity decreasing with increasing temperature (figure S.1A available at stacks.iop.org/Nano/20/255501). The electrical resistance decreased sharply with increasing

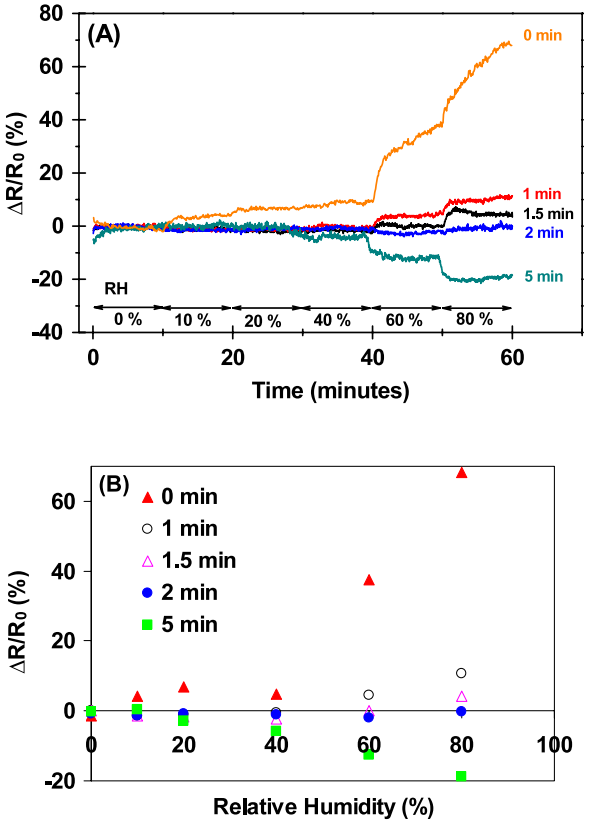

Figure 2. Real-time change of the relative baseline resistance of different PANI(CSA)–SWNTs sensors exposed to increasing relative humidity in the absence of NH_3 (A) and (B) steady state values of the relative resistance change of the baseline resistance as a function of the relative humidity (at 24 °C). The legend shows the PANI deposition time for the different sensors.

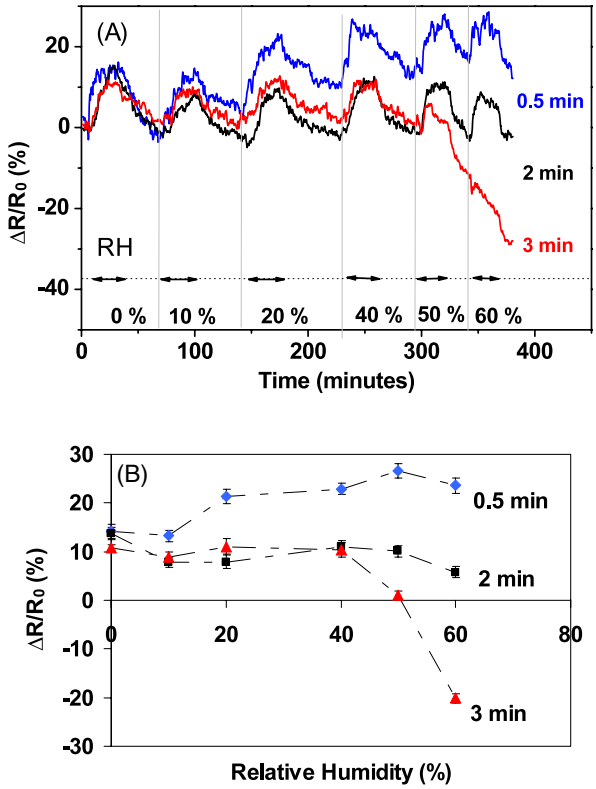

Figure 3. (A) Real-time relative responses of different PANI(CSA)–SWNTs sensors to repeated exposures to 10 ppm_v NH_3 in air at increasing relative humidities (at 24 °C). The arrows indicate the exposure to NH_3. (B) Steady state relative responses of the PANI(CSA)–SWNTs sensors to 10 ppm_v NH_3 in air as a function of the relative humidity. The error bars show the standard deviation of the measurements. The legend shows the PANI deposition time for the different sensors.

temperature indicating that the PANI(CSA)–SWNT network behaved as a typical semiconductor (figure S.1B available at stacks.iop.org/Nano/20/255501).

Figure 2(A) reports the real-time changes in the baseline resistance of the sensors upon exposure to different relative humidities (RH) in air. The results showed that the resistance of the bare carboxylated SWNTs (i.e., functionalized 0 min) dramatically increased in response to exposure to RH, which is consistent with other published results [17–20]. As for the two sensors with the shortest functionalization time (1 and 1.5 min), their resistances slightly increased when the RH was higher than 40%, however, their relative resistance changes (11.3% and 6.4% at 80% RH) were significantly lower than this for bare carboxylated SWNTs. On the other hand, the resistance of the PANI(CSA)–SWNTs with 5 min electrodeposition decreased upon exposure to RH. The steady state values of the baseline resistances at the different RH are reported in figure 2(B). Examination of this figure reveals that the resistance of PANI(CSA)–SWNTs with 2 min electrodeposition time was virtually independent of RH. The reason for this behavior is the opposite electrical response of SWNTs and PANI(CSA) to water vapor. It has been shown by several researchers that H_2O donates electrons to hole charge carriers of p-type SWNTs (0.03 electron per H_2O), thereby increasing the resistance of SWNTs consistent with the observations made for figure 2 [18–20]. Contrary to SWNTs, the resistance of macro-scale PANI(CSA) films decreased upon exposure to H_2O [21, 22], which was explained by the proton exchange-assisted conduction of electrons (PEACE) mechanism [23]. NMR studies indicated that adsorbed H_2O increased the probability of proton exchange, along with redox reactions which change the reduced states (NH_2^+ and NH) to the oxidized state ($NH^+=$ and N=) and results in considerable decrease in the resistivity of PANI [23].

Thus, the opposite electrical responses of SWNTs and PANI(CSA) towards H_2O made it possible to eliminate the effect of RH by having just the right balance of PANI(CSA) functionalization. Examination of the diameter histograms (figures 1(B)) reveals that this balance was achieved when about 10% of the SWNT surface remained unfunctionalized.

To quantify the effect of RH on the response of the sensors to NH_3, three PANI(CSA)–SWNT sensors with different electrodeposition time (0.5, 2, 3 min) were prepared. They were simultaneously and repeatedly exposed to 10 ppm_v NH_3 in air at different relative humidities (figures 3(A) and (B)). Upon exposure to NH_3, a rapid rise in the resistance of all sensors was observed (figure 3(A)). After obtaining a steady state response, the sensors were purged with humid air for recovery. The response to NH_3 was reversible although

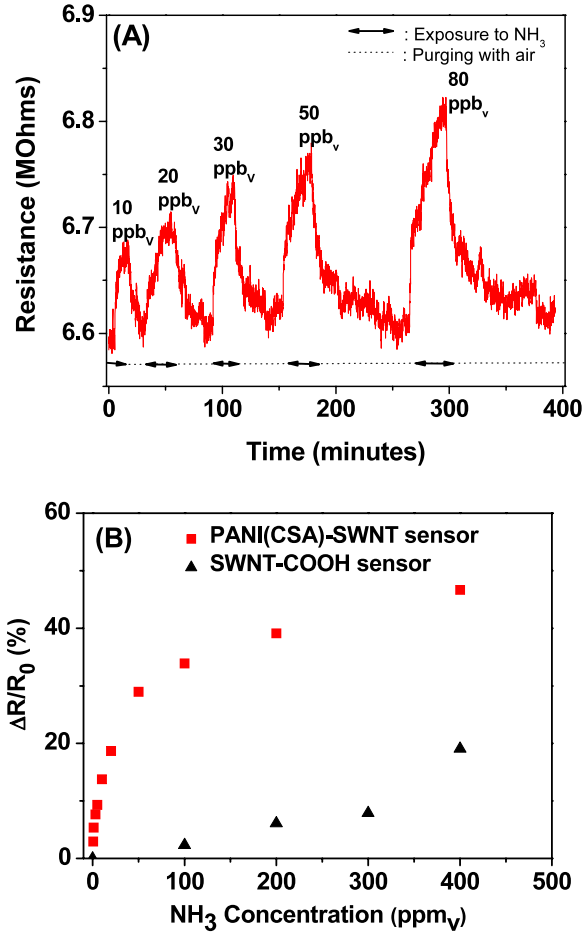

Figure 4. (A) NH_3 gas sensing results using CSA-doped PANI functionalized SWNTs. The arrows show exposure times to NH_3. CSA-doped PANI was electrodeposited at 0.8 V for 2 min. (B) NH_3 relative sensitivity of PANI(CSA)–SWNTs and of carboxylated SWNTs.

recovery was slow compared to other nanomaterials-based sensors [4, 10]. In general, response times ranging from 10 to 30 min have been reported by others for organic polymer functionalized CNT nanosensors [4]. When increasing the RH during NH_3 sensing, the baseline resistance of the sensor with 0.5 min electrodeposition time drifted positively, while there was a general negative drift of the sensor made with 3 min electrodeposition at RH of 50% and above (figure 3(B)). The drift and poor responses of the sensors functionalized with PANI for 0.5 and 3 min as well as the humidity-independent behavior of the sensor functionalized for 2 min are consistent with the results of figures 2(A) and (B) and the observation of opposite responses of SWNT and PANI(CSA) to RH. The sensors functionalized with a suboptimum amount of PANI were affected by moisture, while the optimized sensor was not.

Figure 4(A) shows the humidity-independent sensor's dynamic response to low NH_3 concentrations ranging from 10 to 80 ppb_v at 0% RH while the relative sensitivity of the sensor to NH_3 concentrations up to 400 ppm_v is shown in figure 3(B). The sensitivity of the PANI(CSA)–SWNT sensor was much higher than that of a carboxylated SWNT sensor (figure 4(B)) and similar to that of the best NH_3 nanosensors [4, 11, 13]. The reason for the greater sensitivity lies in the affinity of NH_3 to PANI because of the coordinating roles of the nitrogen atoms of both compounds [16–24], and the deprotonation–protonation process brought by the adsorption–desorption of NH_3. The PANI(CSA)–SWNT exhibited good response repeatability as is illustrated in figure 3(A) for the sensor functionalized 2 min, consistent with earlier results obtained with PANI(Cl)–SWNT nanosensors [16]. Sensor-to-sensor variability was important (±30% change in baseline resistance) due to variability in the sensor making process (results not shown). Cross-interference tests revealed that the optimum PANI(CSA)–SWNT nanosensors were insensitive to at least 1 ppm_v NO_2, 3000 ppm_v H_2, and 1 ppm_v H_2S.

4. Conclusion

In conclusion, we have demonstrated a method to eliminate the cross-interference of a gas analyte on gas nanosensors by accurately controlling the synthesis of the sensing nanomaterial. CSA-doped PANI was precisely electropolymerized onto SWNTs with controlled thickness. The resulting sensors showed excellent sensitivity toward NH_3 at room temperature with minimum interference from H_2O vapor. Overall, these results demonstrate that shortcomings of conventional sensors can be overcome by designing novel nanoengineered materials. The approach of using nanostructures with opposite electrical responses to interferences should be generally applicable to the development of analyte specific nanosensors. The approach paves the way for the development of more selective gas nanosensors.

Acknowledgments

We greatly acknowledge the support of this work from Bourns, Inc., University of California Discovery Grant (UC Discovery), and DOD/DMEA through Center for Nanoscience Innovation for Defense (grant #DOD/DMEA-H94003-06-2-0608).

References

[1] Kong J, Franklin N R, Zhou C W, Chapline M G, Peng S, Cho K J and Dai H J 2000 *Science* **287** 622
[2] Peng S, Cho K J, Qi P F and Dai H J 2004 *Chem. Phys. Lett.* **387** 271
[3] Kolmakov A and Moskovits M 2004 *Annu. Rev. Mater. Res.* **34** 151
[4] Zhang T, Mubeen S, Myung N V and Deshusses M A 2008 *Nanotechnology* **19** 332001
[5] Rumiche F, Wang H H, Hu W S, Indacochea J E and Wang M L 2008 *Sensors Actuators* B **134** 869
[6] Sun Y, Wang H H and Xia M 2008 *J. Phys. Chem.* C **112** 1250
[7] Mubeen S, Zhang T, Yoo B, Deshusses M A and Myung N V 2007 *J. Phys. Chem.* C **111** 6321
[8] Cantalini C, Valentini L, Armentano I, Lozzi L, Kenny J M and Santucci S 2003 *Sensors Actuators* B **95** 195
[9] Gong J W, Chen Q F, Lian M R, Liu N C, Stevenson R G and Adami F 2006 *Sensors Actuators* B **114** 32
[10] Johnson A T C, Staii C, Chen M, Khamis S, Johnson R, Klein M L and Gelperin A 2006 *Semicond. Sci. Technol.* **21** 17

[11] Zhang T, Mubeen S, Bekyarova E, Yoo B Y, Haddon R C, Myung N V and Deshusses M A 2007 *Nanotechnology* **18** 165504
[12] Huyberechts G, Szecówka P M, Roggen J and Licznerski B 1997 *Sensors Actuators* B **45** 123
[13] Li J, Lu Y J, Ye Q, Deltzeit L and Meyyappan M 2005 *Electrochem. Solid State* **8** H100
[14] Delpha C, Siadat M and Lumbreras M 2000 *Sensors Actuators* B **62** 226
[15] Star A, Joshi V, Skarupo S, Thomas D and Gabriel J C P 2006 *J. Phys. Chem.* B **110** 21014
[16] Zhang T, Nix M B, Yoo B Y, Deshusses M A and Myung N V 2006 *Electroanalysis* **18** 1153
[17] Zahab A, Spina L and Poncharal P 2000 *Phys. Rev.* B **62** 10000
[18] Pati R J, Zhang Y M, Nayak S K and Ajayan P M 2002 *Appl. Phys. Lett.* **81** 2638
[19] Huang X J, Sun Y F, Wang L C, Meng F L and Liu J H 2004 *Nanotechnology* **15** 1284
[20] Na P S *et al* 2005 *Appl. Phys. Lett.* **87** 093101
[21] Jain S P, Chakane S J, Samui A B, Krishnamurthy V N and Bhoraskar S V 2003 *Sensors Actuators* B **96** 124
[22] Tarachiwin L, Kiattibutr P, Ruangchuay L, Sirivat A and Schwank J 2002 *Synth. Met.* **129** 303
[23] Travers J P and Nechtschein M S 1987 *Synth. Met.* **21** 135
[24] Debarnot D N and Epaillard F P 2003 *Anal. Chim. Acta* **475** 1

Supplementary Information

Humidity-independent Gas Nanosensor

Ting Zhang[1], Syed Mubeen[1], Bongyoung Yoo[1], Nosang V. Myung[1]* and Marc A. Deshusses[1,2]*

[1]Department of Chemical and Environmental Engineering and Center for Nanoscale Science and Engineering, University of California-Riverside, Riverside, CA 92521

[2]Department of Civil and Environmental Engineering, Duke University, Durham, NC 27708

Supporting Figure

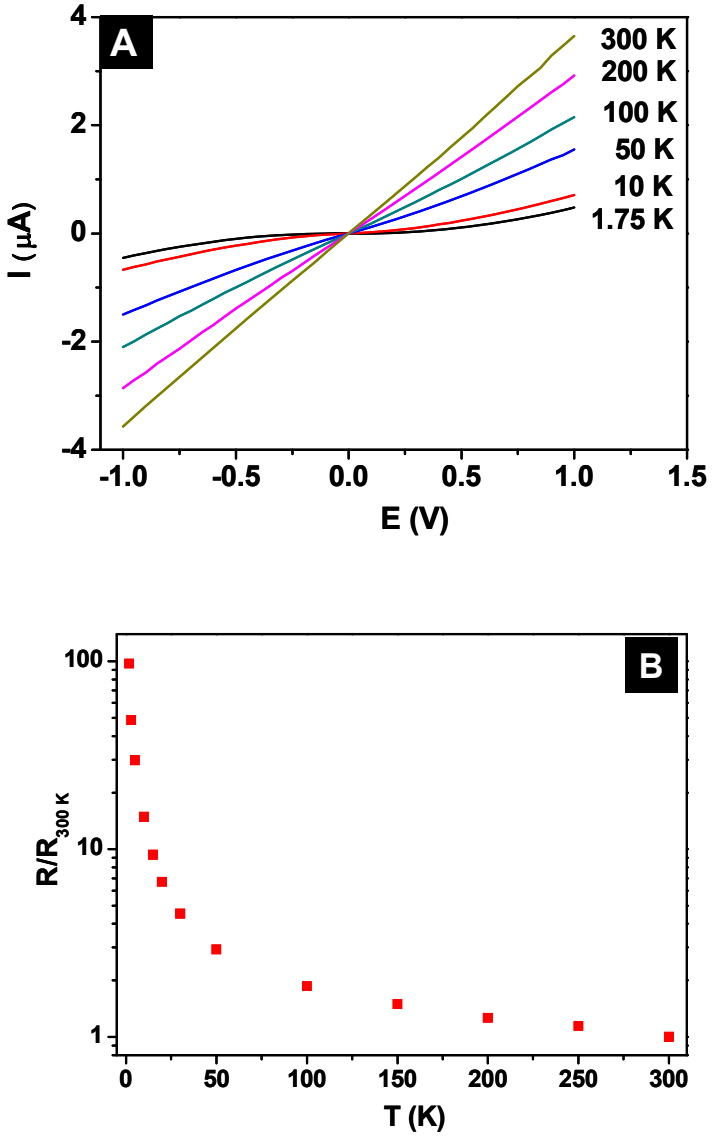

Figure S1 Temperature dependent I-V curves of PANI(CSA)-SWNTs (A) and normalized resistance (B). The deposition time of PANI(CSA) was 2 min.